Original Article

MOLECULAR METABOLISM

Dopamine D2 receptor agonist, bromocriptine, remodels adipose tissue dopaminergic signalling and upregulates catabolic pathways, improving metabolic profile in type 2 diabetes

G. Tavares [1,2,3,4], D. Marques [1], C. Barra [1,2,3], D. Rosendo-Silva [1,2,3], A. Costa [1], T. Rodrigues [1], P. Gasparini [1], B.F. Melo [4], J.F. Sacramento [4], R. Seiça [1,3], S.V. Conde [2,6], P. Matafome [1,2,3,5,*,6]

ABSTRACT

Background and objectives: The therapeutic effects of the dopamine D2 receptor (D2R) agonist, bromocriptine, in type 2 diabetes (T2D) have been attributed to central nervous system actions. However, peripheral dopamine directly modulates glucose uptake in insulin-sensitive tissues and lipid metabolism in adipose tissue (AT). We hypothesized that the dopaminergic system may be impaired in the adipose tissue of patients with T2D and that the therapeutic actions of bromocriptine could involve the modulation of metabolism in this tissue.

Methods: The expression of dopamine receptors was evaluated in visceral AT samples from patients with obesity and stratified in several groups: insulin sensitive (IS); insulin resistance (IR) normoglycaemic; insulin resistant prediabetic; insulin resistant diabetic, according to Ox-HOMA2IR, fasting glycaemia and HbA1c levels. T2D Goto-Kakizaki rats (GK) were fed a high-caloric diet (HCD) for five months and treated with bromocriptine (10 mg/kg/day, i.p.) in the last month. The levels of dopaminergic system mediators and markers of insulin sensitivity and glucose and lipid metabolism were assessed in the peri-epididymal adipose tissue (pEWAT) and brown (BAT) adipose tissues, liver, and skeletal muscle.

Results: Patients with IR presented a decreasing trend of *DRD1* expression in the visceral adipose tissue, being correlated with the expression of *UCP1*, *PPARA*, and insulin receptor (*INSR*) independently of insulin resistance and body mass index. Although no differences were observed in *DRD2, DRD4* expression was significantly decreased in patients with prediabetes and T2D. In HCD-fed diabetic rats, bromocriptine increased D1R and tyrosine hydroxylase (TH) levels in pEWAT and the liver. Besides reducing adiposity, bromocriptine restored GLUT4 and PPARγ levels in pEWAT, as well as postprandial InsR activation and postabsorptive activation of lipid oxidation pathways. A reduction of liver fat, GLUT2 levels and postprandial InsR and AMPK activation in the liver was observed. Increased insulin sensitivity and GLUT4 levels in BAT and an improvement of the overall metabolic status were observed.

Conclusions: Bromocriptine treatment remodels adipose tissue and the liver dopaminergic system, with increased D1R and TH levels, resulting in higher insulin sensitivity and catabolic function. Such effects may be involved in bromocriptine therapeutic effects, given the impaired expression of dopamine receptors in the visceral adipose tissue of IR patients, as well as the correlation of D1R expression with InsR and metabolic mediators.

Keywords Type 2 diabetes; Obesity; Dopamine; Bromocriptine; D2 dopamine receptor; Adipose tissue; Liver

1. INTRODUCTION

Obesity, body mass index (BMI)>30 kg/m^2, is a major cause of morbidity and mortality, associated with an increased risk of metabolic syndrome and type 2 diabetes (T2D) [1,2]. Moreover, insulin resistance (IR) is a core feature of the metabolic syndrome, leading to the development of T2D, dramatically changing glucose and fatty acids metabolism [3]. However, the mechanisms of adipose tissue and liver insulin resistance are still unknown and under investigation.

The D2 receptor (D2R) agonist, bromocriptine, was approved by the Food and Drug Administration (FDA) for the treatment of T2D in USA, given its effects in improving glucose tolerance and insulin sensitivity [4].

[1]Institute of Physiology and Institute of Clinical and Biomedical Research (iCBR), Faculty of Medicine, University of Coimbra, Portugal [2]Center for Innovative Biomedicine and Biotechnology (CIBB), University of Coimbra, Portugal [3]Clinical-Academic Center of Coimbra, Coimbra, Portugal [4]CEDOC, NOVA Medical School, Faculdade de Ciências Médicas, Universidade Nova de Lisboa, Lisboa, Portugal [5]Instituto Politécnico de Coimbra, Coimbra Health School, Coimbra, Portugal

[6] Silvia V. Conde and Paulo Matafome are both senior authors of this manuscript.

*Corresponding author. Faculty of Medicine, Pole III of University of Coimbra, Subunit 1, 1rst floor, Azinhaga de Santa Comba, Celas, 3000-354, Coimbra, Portugal. Fax: +351239480034. E-mail: paulo.matafome@uc.pt (P. Matafome).

Received February 3, 2021 • Revision received April 5, 2021 • Accepted April 22, 2021 • Available online 29 April 2021

https://doi.org/10.1016/j.molmet.2021.101241

Abbreviations

AMPK	AMP-activated protein kinase
AMPK-Thr172	Phosphorylated AMP-activated protein kinase on 172 threonine residue
BAT	Brown adipose tissue
DARPP 32	Dopamine- and cAMP-regulated neuronal phosphoprotein
DRD1	Gene encoding for human dopamine receptor 1
DRD2	Gene encoding for human dopamine receptor 2
DRD4	Gene encoding for human dopamine receptor 4
D1R	Dopamine receptor 1
D2R	Dopamine receptor 2
GLUT2	Glucose transporter 2
GLUT4	Glucose transporter 4
HCD	High caloric diet
INSR	Gene encoding for human insulin receptor
InsR	Insulin receptor
InsR-Tyr1361	Phosphorylated insulin receptor on 1361 tyrosine residue
IR	Insulin resistance
IS	Insulin sensitive
T2D	Type 2 Diabetes
TH	Tyrosine hydroxylase
pEWAT	peri-epididymal adipose tissue
PPARA	Gene encoding for human peroxisome proliferator-activated receptor alfa
PPARγ	Peroxisome proliferator-activated receptor gamma
UCP1	Gene encoding for human uncoupling protein 1
VAT	Visceral adipose tissue

Bromocriptine-QR appears to be a unique insulin sensitizing therapy with a good safety profile, without risk of weight gain or hypoglycaemia and with a potential to reduce adverse cardiovascular risk [4,5]. Moreover, it also presents important pharmacological advantages, such as lower side effects, safety, tolerability, and good adherence to treatment [5–7]. Bromocriptine acts on pancreatic beta cells to downregulate glucose-stimulated insulin secretion (GSIS), avoiding long-term beta cell exhaustion [8]. On the other hand, it also has positive effects on insulin sensitivity, which have been attributed to the regulation of the hypothalamic sympathetic output and prolactin secretion [6,9]. Nevertheless, the existence of functional dopamine receptors in adipose tissue suggests that this drug may exert direct regulatory functions in this tissue [10]. Although catecholamines have well-known lipolytic effects in the adipose tissue, recent evidences support the theory that bromocriptine also acts on adipose tissue to modulate insulin action and glucose and fatty acid metabolism [11]. Accordingly, we have recently observed that peripheral dopamine stimulates glucose uptake *in vivo* in insulin-sensitive tissues, such as the adipose tissue, liver and skeletal muscle, and bromocriptine directly acts in the same tissues to regulate, not only glucose uptake, but also insulin sensitivity and metabolic function [12]. Despite these direct and new effects of bromocriptine that we described, the effects of chronic bromocriptine stimulation in such tissues have never been addressed before, as well as the role of local dopaminergic signalling. Therefore, revealing bromocriptine peripheral actions on insulin-sensitive tissues may enable to identify new therapeutic targets and strategies in T2D.

Given the current knowledge of direct dopamine effects in adipose tissue, in this study, our first objective was to evaluate the expression of dopamine receptors in the visceral adipose tissue of patients with metabolic syndrome and correlate it with markers of adipocyte metabolism. Additionally, our second aim was to investigate the effects of chronic bromocriptine treatment in an animal model of T2D fed a hypercaloric diet (HCD) in remodelling adipose tissue dopaminergic signalling, insulin sensitivity, and metabolic function.

2. RESEARCH DESIGN AND METHODS

2.1. Human study

A cohort of obese patients aged 25–65 years old (diabetic and non-diabetic) was selected at the obesity surgery appointment at the Hospital Geral de Coimbra (Covões) - Centro Hospitalar Universitário de Coimbra. All subjects signed an informed consent and the study was approved by the institutional ethics committee (Ethics Committee of the Coimbra University Hospital Centre), according to the principles outlined in the Declaration of Helsinki. Exclusion criteria were as follows: active inflammatory and chronic diseases (neurodegenerative diseases or active tumours), previous restrictive (sleeve gastrectomy) or mal-absorptive (gastric bypass or duodenal switch) surgeries and T2D medication other than metformin (GLP-1RA, DPPIV inhibitors or insulin). On the day before surgery, height and body weight were recorded and fasting blood samples were collected for biochemical analysis. Visceral white adipose tissue samples were collected during surgery and kept in liquid nitrogen to be then stored at - 80 °C.

2.2. Patient selection and characterization

Ninety-two obese patients (77 women and 15 men) were divided in groups according to glycaemic profile: fasting glucose levels, HbA1c, and Ox-HOMA2IR. Subject characterization resulted in four different groups: 1 – insulin sensitive group (IS) ($n = 17$), composed by individuals that were both IS and normoglycaemic (NG) (Ox-HOMA2IR < 1); 2 – insulin resistant (IR) and NG group ($n = 29$), with insulin resistant patients (Ox-HOMA2IR>1) that were normoglycaemic (fasting glucose$<$100 mg/dL and HbA1c$<$5.7%); 3 – prediabetic group ($n = 28$), that allocated IR patients with fasting glucose levels from 100 to 125 mg/dL or HbA1c between 5.7 and 6.4%; 4 – T2D group ($n = 18$), constituted by IR subjects diagnosed with T2D (fasting blood glucose$>$125 mg/dL or HbA1c$>$6.4%) (Supplementary Table 1) [13].

2.3. RNA extraction

Total RNA was extracted from VAT human biopsies (100 mg) using an RNeasy Lipid Tissue Mini Kit (Qiagen, Germany). RNA samples were analysed by NanoDrop One/One spectrophotometer (Thermo Fisher Scientific, Waltham, MA, USA) at 260 nm to evaluate its concentration. RNA integrity was also analysed through capillary electrophoresis with an Agilent RNA 6000 Nano Kit and the results obtained with the Agilent 2100 Bioanalyser (Agilent Technologies, CA, USA).

2.4. Quantitative real-time polymerase chain reaction using the high throughput platform biomark$_{tm}$ HD system

RNA sample was diluted into the same concentration (25 ng/μL). Reverse transcriptase enzyme [qScript cDNA super mix (Quanta BioSciences)] was added to each RNA sample to obtain cDNA. To amplify cDNA samples, they were mixed with a mix of pooled primers (500 nM final concentration each), with a PreAmp Master Mix enzyme (Fluidigm), following 12 cycles of thermal cycling according to the enzyme manufacturer. Samples were then treated with Exonuclease I (New

England Biolabs) to remove unincorporated primers and were diluted 5 × in TE buffer (10 mM Tris—HCl, 1 mM EDTA). For each sample a Pre-Mix was prepared (SsoFast Eva Green Supermix, BioRad), with DNA binding dye sample reagent at 20 × (Fluidigm). Thereafter, samples were pipetted into the respective inlet of a Fluidigm® 96.96 Gene expression IFC. For each gene assay, a mix with 2 × Assay loading reagent (Fluidigm), forward and reverse primers (50 μM stock) diluted TE buffer was individually prepared. The primers sequences were: *DRD1* forward- ACACAATTAACTCCGTTTCC and reverse- GTAGTGTCCCTGTTTGATTG; *DRD2* forward- TCCACTAAAGGGCAACTG and reverse- GGAAACTCCCATTAGACTTC; *DRD4* forward- CATCTACACTGTCTTCAACG and reverse- ATTAACGTACAAAAGCGCC; *UCP-1* forward- ACAGCACCTAGTTTAGGAAG and reverse- CTGTACGCATTATAAGTCCC; *PPARA* forward- CCTAAAAAGCCTAAGGAAACC and reverse- GATCTCCACAGCAAATGATAG; and *INSR* forward- GATCCAATCTCAGTGTCTAAC and reverse- CCTTTGAGGCAATAATCCAG, obtained by Sigma Aldrich, (USA) and reconstituted in water to a final concentration of 100 μM. Then each gene assay was pipetted into their respective assay inlets on the chip and loaded with the Load mix (136 ×) script of the HX controller (HD Biomark), using the BioMark HDTM, accordingly to the cycling parameters recommended by Fluidigm® for 96.96 Gene expression Integrated Fluidic Circuit. Then data were collected with Data Collection Software and analysed using Fluidigm® Real Time PCR Analysis v2.1 software. All data were normalized for the reference gene *ATCB*.

2.5. Animal study

Wistar rats from our breeding colonies (Faculty of Medicine, University of Coimbra) were kept under standard conditions [13,14]. The experimental protocol was approved by the local Institutional Animal Care and Use Committee (ORBEA 04—2015), and all the procedures were performed by licensed users of Federation of Laboratory Animal Science Associations (FELASA) and in accordance with the European Union Directive for Protection of Vertebrates Used for Experimental and Other Scientific Ends (2010/63/EU). At 1 month of age, type 2 diabetic GK rats were divided into two groups; the first group was maintained with the same standard diet until 6 months of age (A03; 5% triglycerides and 45% carbohydrates, SAFE, France) (GK group, n = 33), while the other group was fed a high-caloric diet (HCD) in the same period (customized A03 HCD with 20% fat plus 20% sucrose, SAFE, France) to induce weight gain. The HCD-fed group was randomly divided into three groups: the first group without further treatment apart from the diet (GKHCD, n = 20), the second group with bromocriptine treatment in the last month (GKHCDBr, n = 17), and the third group with vehicle administration during the same period (GKHCDVh, n = 15). Male Wistar rats fed with a standard diet for 6 months were used as control (n = 22). Bromocriptine gently supplied by Generis®, (Amadora, Portugal) was diluted 1:4 DMSO/H_2O and administered daily via intraperitoneal (i.p) injection (10 mg/kg/day) during the last month. In the vehicle group, the same volume (100 μL) of the vehicle 1:4 DMSO/H_2O was administered i.p. during the same period.

2.6. Insulin tolerance teste

Two days prior to the sacrifice, an intraperitoneal insulin tolerance test (IPITT) was performed. Fasted (6 h) animals were injected with insulin (0.25 U/kg, Lilly, Portugal) and glucose was measured before and after 15, 30, 60, and 120 min using a Glucometer (Bayer, Germany). The area under the curve was then calculated.

2.7. Blood sampling and tissue collection

On the day of the sacrifice, fasting (6 h) glycaemia, triglyceridemia, and cholesterol levels were measured in the blood sample obtained from the tail vein by using a Glucometer (Bayer, Germany) and the Accutrend system (Roche, Germany) with the respective reactive test stipes. Before sacrifice, the animals were divided into 2 subgroups, those sacrificed after 6 h fasting — "postabsorptive" (WSD = 15, GKSD = 21, GKHCD = 13, GKHCDBr = 11, GKHCDVh = 9) and those sacrificed 1 h after a mixed meal ingestion — "post-prandial" (WSD = 7, GKSD = 12, GKHCD = 7, GKHCDBr = 6, GKHCDVh = 6). Then, the animals were anesthetized with ketamine chloride (75 mg/kg, Nimatek, Dechra, UK) and chlorpromazine chloride (2.65 mg/kg, Lab. Vitória, Portugal).

In the set of animal sacrificed after 6 h fasting, plasma, and serum samples were collected by cardiac puncture as previously described [13,15] for further evaluation of insulin, glucagon, leptin, adiponectin, and free fatty acid levels. The animals were sacrificed by cervical displacement, and peri-epididymal adipose tissue (pEWAT), brown adipose tissue (BAT), muscle, and the liver were collected, weighted and stored in 4% formalin solution or at −80 °C. In the set of animals sacrificed after a mixed meal, 3 mL of Nutricia, Fortimel (Nestle, Switzerland) was administered through gavage and animals were sacrificed 1 h later for tissue collection.

2.8. Western blotting

Tissues were homogenized as previously described [13,14] and samples were loaded in 8% polyacrylamide gels, separated by SDS-PAGE and transferred to a PVDF membrane (Advansta, USA). Membranes were incubated with the specific primary antibodies overnight at 4 °C (listed below), and then incubated 2 h at room temperature with secondary antibodies. The secondary antibodies were anti-mouse (GE Healthcare, UK), anti-rabbit and anti-goat (Bio-Rad, USA). Membranes were revealed using ECL substrate in a Versadoc system (Bio-Rad, USA) and analysed with Image Quant® (Molecular Dynamics, USA).

2.9. Reagents, ELISA kits and antibodies

Salts and organic solvents used in solution preparations were purchased from Thermo Fisher Scientific (Leicestershire, UK), Sigma Chemicals (United States of America - USA) or Merck Darmstad (Germany), with the highest grade of purity commercially available. Antibodies used were AMPK (#2532), AMPK-Thr172 (#2535 GLUT 4, PPARγ (#2213S and #2443S, Cell Signaling, USA), InsRβ (sc-57342, Santa Cruz Biotechnology, USA), GLUT2 (ab54460) and InsR-Tyr1361 (ab60946, Abcam, UK). Antibodies D1R, D2R, DARPP32, DARPP32-Thr34 and tyrosine hydroxylase (TH) were also used (ab81296, ab85367, ab40801 and ab51114 respectively, Abcam, UK; T1299, Sigma Aldrich, USA). Calnexin was used as loading control (AB0037, Sicgen, Portugal). Plasma insulin levels were assessed through the Rat Insulin ELISA Kit, (Mercodia, Sweden), plasma glucagon using the ELISA Kit (Wako, Germany), and plasma levels of leptin and adiponectin were measured using the Mouse/Rat Leptin Quantikine ELISA Kit and Rat Total Adiponectin/Acrp30 Immunoassay (R&D system, USA). Free fatty acids were assessed using the FFA Assay Kit (ZenBio, NC, USA). Furthermore, 100 mg of liver samples were homogenised in the lysis buffer (1 mL of 5% NP-40/ddH_2O solution) and hepatic triglycerides content was quantified by the colorimetric Triglyceride Quantification Assay Kit (Abcam 65336, UK). Moreover, 30 mg of pEWAT were homogenised in PBS 0.02 M, pH 7.2 (BAM R61, FDA) to quantify β-hydroxybutyrate by a colorimetric assay (Biovison K632-100, USA).

2.10. Statistical analysis

Non-parametric tests were performed on the clinical human data (sample size < 30/group), and results were presented as median and interquartile range. Kruskal–Wallis and Mann–Whitney tests were used to compare gene expression between groups according to its division. Spearman correlation test was performed to assess correlation between variables. In the animal study, results were presented as mean $\pm$ standard deviation. One-way ANOVA test with Tukey's multiple comparisons was used to performed systemic parameters analysis and total proteins quantification. For phosphorylated proteins, Kruskal–Wallis test (all pairwise multiple comparisons) was applied to determine statistical differences between the groups. Differences were considered significant at $p < 0.05$. All computation analyses were performed using Graphpad Prism (6.0 version, USA).

3. RESULTS

3.1. Expression of dopamine receptors is impaired in the visceral adipose tissue of patients with insulin resistance

Patients included in the diabetic group (fasting blood glucose>125 mg/dL or HbA1c>6.4%), were previously shown to have a failure of beta-cell function, and lower levels of high density lipoprotein cholesterol and adiponectin, markers of adipose tissue dysfunction [13]. Detailed clinical characterization of the groups is described in Supplementary

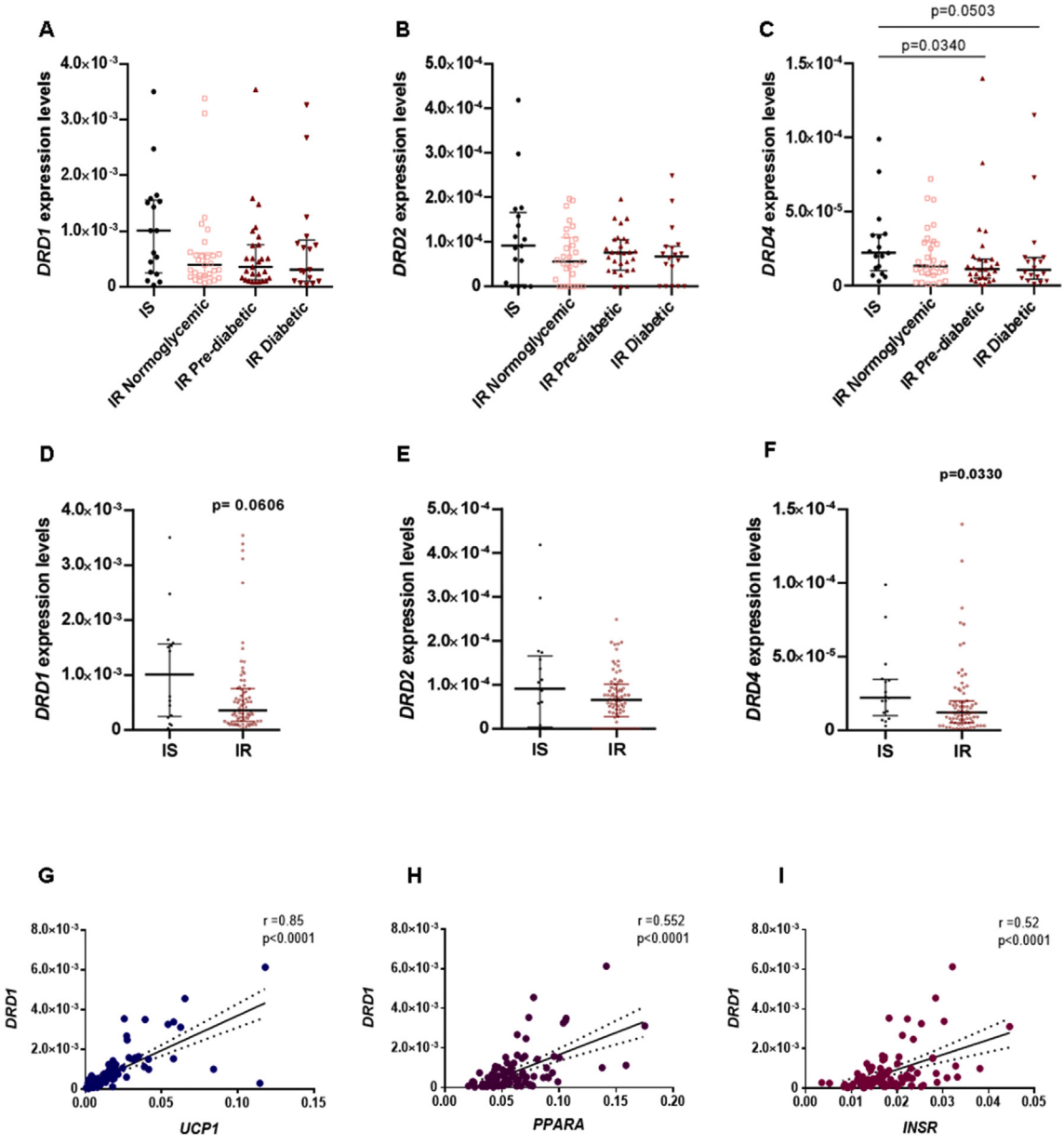

Figure 1: Expression of dopamine receptor in visceral adipose tissue (VAT) of patients with metabolic syndrome. Upper line shows VAT expression of DRD1 (A), DRD2 (B) and DRD4 (C) in each group of patients: insulin-sensitive (IS), and insulin resistant (IR) normoglycemic, prediabetic, and type 2 diabetic patients. All IR patients were grouped and compared with IS patients for DRD1 (D), DRD2 (E) and DRD4 (F). Bottom line shows the correlations between DRD1 expression and UCP-1(G) and PPARA (H) and the insulin receptor INSR (I). Values are median $\pm$ interquartile range. Kruskal–Wallis and Mann–Whitney tests were used to analyse gene expression data according to the patient's group. Spearman's correlation test was used to performed correlation analysis.

Table 1. Here, we investigated the gene expression of dopamine receptors in the adipose tissue of these patients and correlated their expression with markers of adipocyte metabolic function. Expression of *DRD1*, *DRD2* and *DRD4* was evaluated in the four groups of patients, showing decreased *DRD4* expression in patients with prediabetes and T2D when compared with IS patients ($p < 0.05$, Figure 1C). No significant differences were observed for *DRD1* and *DRD2* expression (Figure 1A–C), and no expression was detected for *DRD3* and *DRD5*. Importantly, *DRD1* expression was 10-fold higher than that of the other dopamine receptors (Figure 1A). In order to evaluate the relation between insulin resistance (IR) and dopamine receptor expression, all IR patients (groups 2, 3, and 4) were compared to IS patients, as depicted in Figure 1 (D, E, F). Decreased *DRD4* expression in patients with IR was also observed when comparing to IS patients (Figure 1F, $p < 0.05$). Despite no differences were observed for *DRD2* expression, a trend to decreased *DRD1* expression ($p = 0.06$) was observed in IR patients when compared to IS individuals. In order to understand the possible involvement of dopamine receptors in regulating adipocyte metabolism, the correlation between *DRD1* expression with *INSR* and genes involved in lipid metabolism was determined. Figure 1 shows a positive correlation between *DRD1* expression and *UCP-1* ($p < 0.001$, $\rho = 0.85$) (G), *PPARA* ($p < 0.001$, $\rho = 0.55$) (H) and *INSR* expression ($p < 0.001$, $\rho = 0.52$) (I). Importantly, the expression of *UCP-1*, *PPARA* and *INSR* was also decreased in diabetic patients, suggesting that the impairment of adipose tissue dopaminergic signalling is correlated with impaired insulin sensitivity and metabolic function (data not shown). Multiple regression analysis has shown that the correlations of D1DR with UCP-1, PPAR and INSR are independent of IR and BMI (Supplementary Fig. 1).

3.2. Bromocriptine treatment increases D1R expression in pEWAT and the liver in an animal model of T2D and obesity

Although previous evidences indicate the central actions of bromocriptine, recent findings suggest a direct action of dopamine and bromocriptine in peripheral insulin-sensitive tissues [12]. In order to understand the role of bromocriptine treatment in regulating dopaminergic signalling in insulin-sensitive tissues, the protein levels of D1R, D2R, the downstream effector DARPP32 and tyrosine hydroxylase (TH) were determined in pEWAT, the liver, BAT and soleus muscle. Figure 2A shows decreased D1R levels in pEWAT of GK rats feeding a standard or a HCD (GKHCD) ($p < 0.05$), similarly to what is observed in human adipose tissue in Figure 1. Bromocriptine treatment significantly improved D1R levels ($p < 0.01$ vs GKSD and vs GKHCD) to levels similar to that in Wistar control animals. TH levels were also increased in treated animals, suggesting higher local dopamine production (Figure 2C, $p < 0.05$ vs GK and GKHCD). Similarly, in the liver, D1R (Figure 2D, $p < 0.05$ vs GK and GKHCD) and TH levels (2F, $p < 0.05$ vs GK, GKHCD and GKHCDVh) were increased after bromocriptine treatment. On the other hand, D2R and DARPP32 levels were not altered among groups in both tissues (Figure 2B,E, representative western blot images in the right panel). No significant changes in dopaminergic receptors and TH levels were observed in BAT and skeletal muscle (representative western blot images at Figure 2 G and H).

3.3. Bromocriptine increases insulin sensitivity and drives metabolic pathways towards lipid oxidation in pEWAT

In order to understand the impact of dopaminergic system remodelling induced by bromocriptine in pEWAT, markers for the endocrine and metabolic function of adipose tissue were evaluated. As shown in Figure 3, HCD-fed GK rats (GKHCD and GKHCDVh) exhibited increased epididymal fat mass (Figure 3B) and adipocyte volume (Figure 3C) compared to GK rats fed a standard diet (GKSD, $p < 0.01$). Bromocriptine significantly decreased epididymal fat mass (Figure 3B) ($p < 0.05$ vs GKHCD and $p < 0.01$ vs GKHCDVh) and adipocyte size (Figure 3C) ($p < 0.05$ vs GKDS, $p < 0.0001$ vs GKHCD and GKHCDVh). Representative haematoxylin-eosin images are shown in Figure 3A and it is clear from the images the effect of bromocriptine in decreasing adipocyte size. Decreased adiposity in GKHCDBr rats was accompanied by lower plasma leptin levels (Figure 3D, $p < 0.001$ vs GKHCD and $p < 0.0001$ vs GKHCDVh), while adiponectinemia remained unchanged between groups (Figure 3E) (see Figure 4).

Concerning insulin sensitivity and metabolic pathways, bromocriptine treatment increased GLUT4 (Figure 3F, $p < 0.001$ vs WSD, GKSD, GKHCD and GKHCDVh), insulin receptor (InsR) (Figure 3G, $p < 0.001$ vs GKSD and $p < 0.0001$ vs GKHCD) and PPARy (Figure 3I, $p < 0.001$ vs GKSD, $p < 0.001$ both vs GKHCD and GKHCDVh), while no differences were observed in total AMPK levels between groups (Figure 3H). The activation of the InsR and AMPK was determined in postabsorptive and post-prandial states. In the postabsorptive stage (6 h fasting), no differences were found between groups regarding InsR activation (IR-Tyr1361, Figure 3J). Nevertheless, increased levels of AMPK-Thr172 (Figure 3K, $p < 0.05$ vs GKSD) and a trend to increase ATP citrate lyase (ACL-Ser455, Figure 3L, $p = 0.056$ vs GKSD) were found in pEWAT after bromocriptine treatment. Such results suggest increased catabolic activity, and particularly lipid oxidation, which was confirmed by the increase in β-hydroxybutyrate levels in pEWAT ($p < 0.01$ vs WSD, $p < 0.001$ vs GKSD, $p < 0.01$ vs GKHCD and $p < 0.05$ vs GKHCDVh) by bromocriptine treatment (Figure 3M), while no differences were found in the serum (data not shown). Increased catabolic activity is thought to reduce lipotoxicity and IR. Accordingly, in the post-prandial state, bromocriptine increased IR-Tyr1361 levels (Figure 3N, $p < 0.05$ vs GKHCD), while AMPK-Thr172 levels remained similar to the other groups (Figure 3O).

3.4. Bromocriptine reduces liver triglyceride content without activating liver AMPK pathway

Figure 4A shows liver haematoxylin-eosin staining for the different studied groups. A high amount of lipid droplets consistent with hepatic steatosis phenotype was observed in animals fed with a HCD (Figure 4A, GKHCD and GKHCDVh), consistent with the observed increase in liver weight (Figure 4B, $p < 0.001$ vs WSD and GKSD) and triglyceride content (Figure 4C, $p < 0.001$ vs WSD and GKSD). Bromocriptine notably reduced the presence of lipid droplets in the haematoxylin-eosin staining and reversed hepatic steatosis (Figure 4A), which was accompanied by decreased liver weight (Figure 4B, $p < 0.001$ vs GKHCD) and hepatic triglycerides (Figure 4C, $p < 0.01$ vs GKHCD and GKHCDVh).

In order to understand the role of bromocriptine in the regulation of hepatic metabolic function, InsR and AMPK activation, as well as GLUT2 levels were determined. Animals treated with bromocriptine showed increased total InsR levels (Figure 4E, $p < 0.05$ vs GKSD $p < 0.01$ vs GKHCD) but no changes in AMPK (Figure 4F). Intriguingly, lower levels of GLUT2 were also observed after bromocriptine treatment (Figure 4D, $p < 0.001$ vs WSD, $p < 0.01$ vs GKSD and $p < 0.01$ vs both GKHCD and GKHCDVh), as well as lower InsR-Tyr1361 (Figure 4I, $p < 0.05$ vs GKHCD) and tendentially lower AMPK-Thr172 levels (Figure 4J, $p = 0.07$ vs GKSD) in the post-prandial state. No differences were observed in InsR-Tyr1361 and AMPK-Thr172 levels in the postabsorptive state (Figure 4G,H).

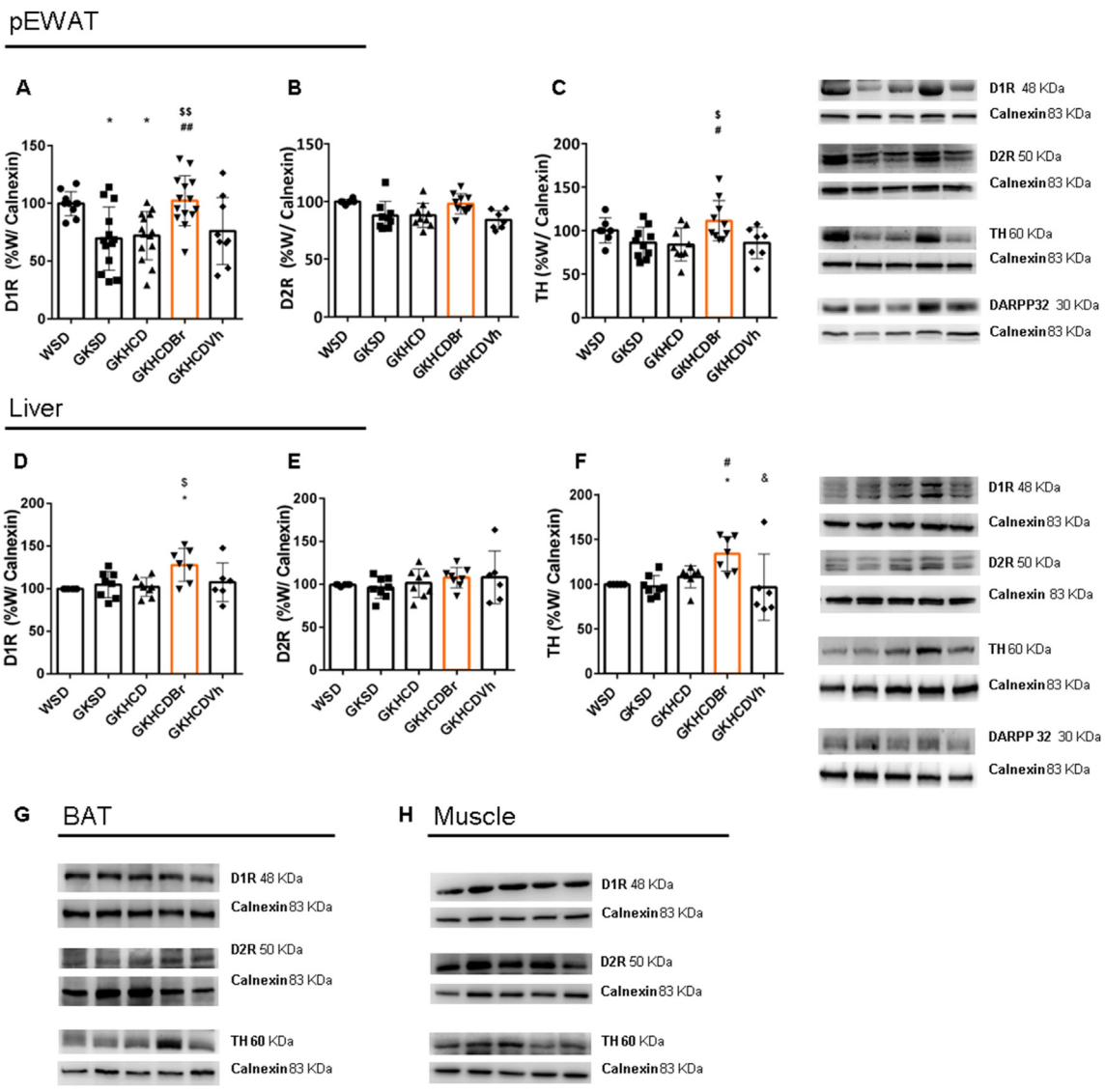

Figure 2: Alterations of dopaminergic signalling in peri-epididymal adipose tissue (pEWAT) and liver after bromocriptine treatment in an animal model of type 2 diabetes and obesity. Increased dopamine D1 receptor (D1R) (A) and tyrosine hydroxylase (TH) (C) in the pEWAT, while no differences were observed for dopamine D2 receptor (D2R) (B). Similar results were observed for D1R (D), D2R (E) and TH (F) in the liver. Representative western blot images are shown in the right panel. The bottom line shows representative western blot images from dopaminergic signalling in the brown adipose tissue (BAT) (G) and the skeletal muscle (H), where no differences were found between groups. Bars represent means ± standard deviation. Differences between groups were assessed by one-way ANOVA with Tukey's multiple comparisons. * Different from WSD; # different from GKSD; $ different from GKHCD; & different from GKHCDBr. *$p < 0,05$; **$p < 0,01$; ***$p < 0.001$.

3.5. Bromocriptine increased fasting insulin signalling in brown adipose tissue but has no effects in the skeletal muscle

Although bromocriptine did not change the BAT dopaminergic system, increased GLUT4 levels were observed after the treatment (Figure 5A, $p < 0.001$ vs WSD, $p < 0.01$ vs GKSD, $p < 0.001$ vs GKHCD and $p < 0.05$ vs GKHCDVh), while both total levels of IR and AMPK remained similar between groups (Figure 5B,C). Furthermore, bromocriptine also increased postabsorptive levels of InsR-Tyr1361 (Figure 5D $p < 0.05$ vs GKHCD), but not AMPK-Thr172 (Figure 5E). Animals sacrificed at the post-prandial stage presented similar levels of InsR-Tyr1361 (Figure 5F) and AMPK-Thr172 (Figure 5G) between groups. In the skeletal muscle, GLUT4, InsR, and AMPK levels did not change between groups (Figure 5H–J). Moreover, either postabsorptive or post-prandial InsR-Tyr1361 and AMPK-Thr172 levels also remained similar between groups (Figure 5K–N).

3.6. Improved adipose tissue insulin sensitivity and metabolic function after bromocriptine treatment is associated with better metabolic profile

In accordance with previous reports from our laboratory [16], GK rats naturally present lower body weight than Wistar rats (Figure 6A and 6A1; $p < 0.001$). HCD-fed GK rats showed higher weight gain in the last month (Figure 6B $p < 0.05$ vs GKSD), which was associated with increased caloric intake during the same period of time (Figure 6C $p < 0.001$, WSD vs GKHCD and GKSD vs GKHCD; $p < 0.01$ WSD vs and $p < 0.001$ GKSD vs both GKHCD and GKHCDVh). On the

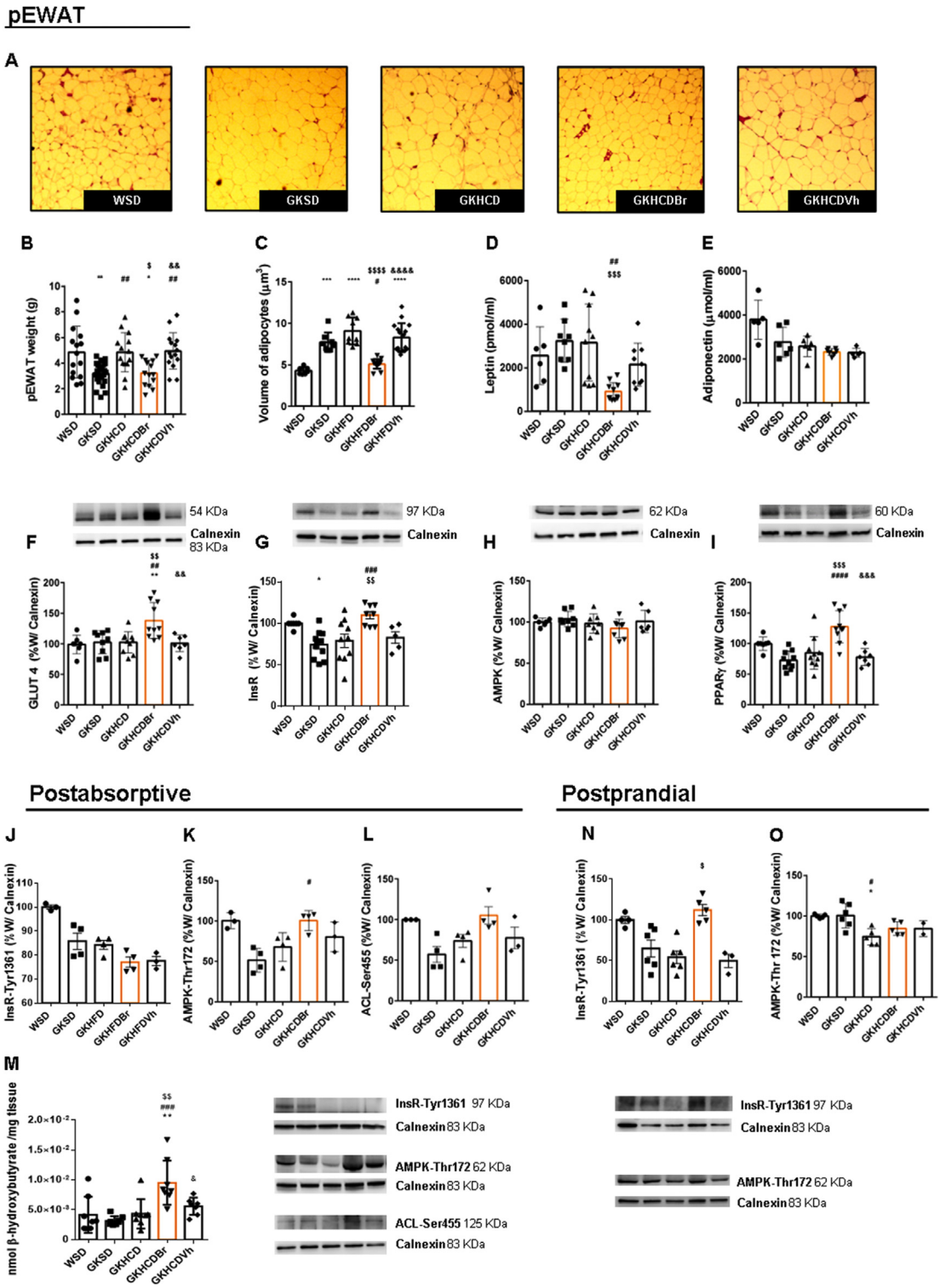

Figure 3: Improvement of insulin sensitivity and remodelling of adipose tissue catabolic pathways by Bromocriptine. Haematoxylin-eosin staining (A, 100 ×) of peri-epididymal adipose tissue (pEWAT). Bromocriptine treatment decreased pEWAT weight (B), adipocytes volume (C) and plasma leptin levels (D), while no changes were observed for plasma adiponectin levels (E). Bromocriptine treatment increased glucose 4 transporter (GLUT4) (F), insulin receptor (InsR) (G) and Peroxisome proliferator-activated receptor gamma (PPARγ, H), while AMP-activated protein kinase (AMPK, I) remained similar between groups. In the bottom panel, no changes were observed in postabsorptive activation of InsR (InsR-Tyr1361, J), but Bromocriptine increased AMPK-Thr172 (K), ACL-Ser455 (L) and β-hydroxybutyrate levels (M). In the post-prandial stage, the InsR was more activated (, N), while no differences were found AMPK activation (O) in Bromocriptine-treated rats. Bars show means ± standard deviation. One-way ANOVA with Tukey's multiple comparisons was used to assess differences between groups. Kruskal–Wallis test was used to analyse InsR-Tyr1361 and AMPK-Thr172. * Different from WSD; # different from GKSD; $ different from GKHCD; & different from GKHCDBr. Level of significance: *p < 0,05; **p < 0,01; ***p < 0.001.

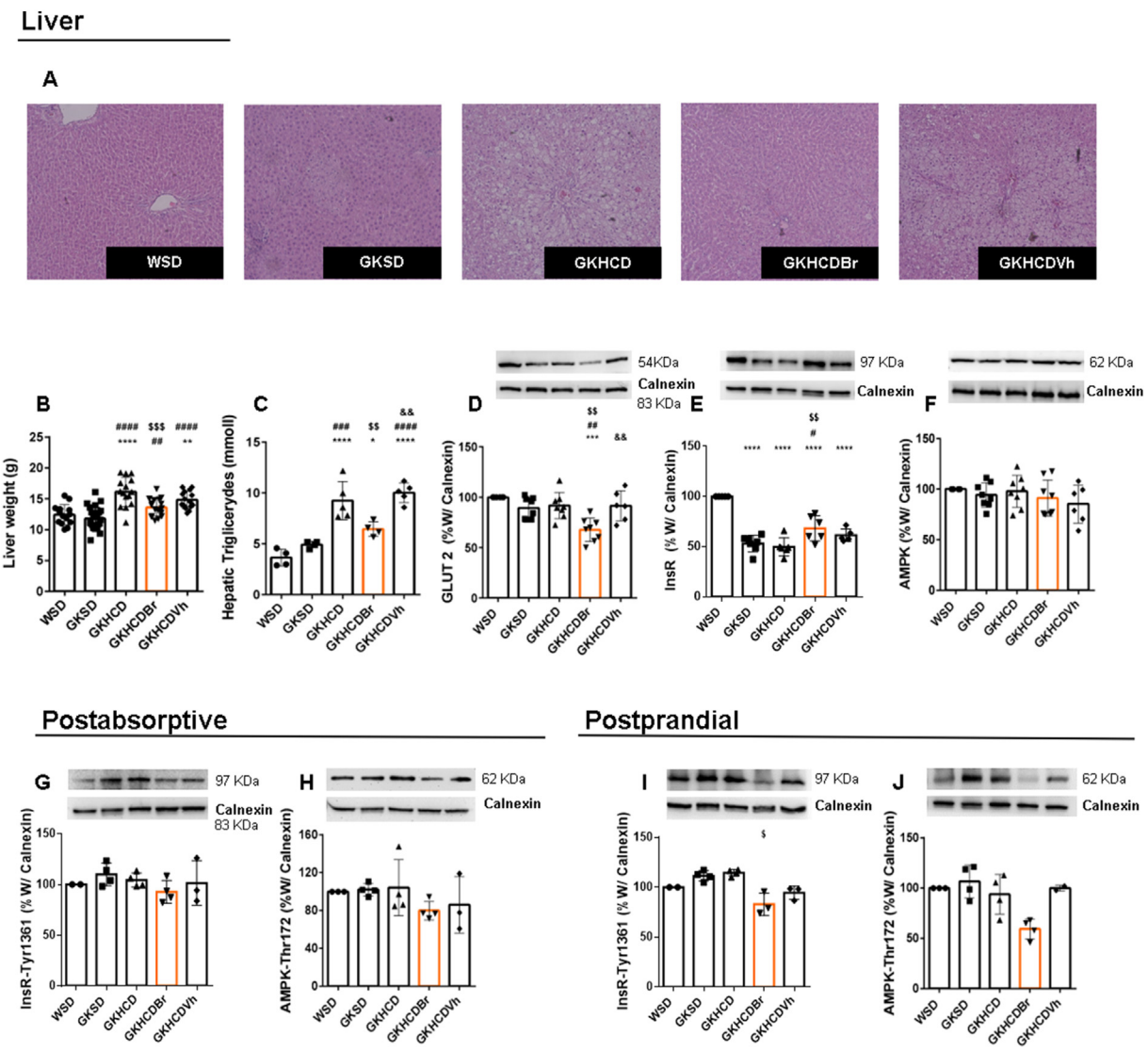

Figure 4: Bromocriptine reduces liver triglycerides content without activating liver AMPK pathway. Liver haematoxylin-eosin staining (A, 100 $\times$) showing a reduction of hepatic steatosis after bromocriptine treatment, in accordance with lower liver weight (B) and hepatic triglycerides (C). Bromocriptine treatment decreased GLUT2 (D), but increased InsR (E), while AMPK (F) levels did not alter between groups. No changes were observed in InsR-Tyr1361 (G) nor AMPK-Thr172 (H) in the postabsorptive stage. Postprandially lower levels of InsR-Tyr1361 (I) and no changes in AMPK-Thr172 (J) were observed. Bars represent means $\pm$ standard deviation. One-way ANOVA was used for liver weight, hepatic triglycerides, GLUT2, InsR and AMPK; Kruskal–Wallis test was used for InsR-Tyr1361 and AMPK-Thr172. *Different from WSD; # different from GKSD; $ different from GKHCD; & different from GKHCDBr. Level of significance: *$p < 0.05$; **$p < 0.01$; ***$p < 0.001$.

other hand, bromocriptine treatment has been shown to prevent weight gain (Figure 6A2 and 6B, $p < 0.001$ vs GKHCD and $p < 0.05$ vs GKHCDVh) and decrease the caloric intake (Figure 6C, $p < 0.0001$ vs GKHCD and GKHCDVh).

The increased body weight and caloric intake in HCD-fed rats was followed by increased fasting plasma triglycerides (Figure 6D, $p < 0.0001$, WSD vs GKHCD and $p < 0.001$ WSD vs GKHCDVh; $p < 0.0001$, GKSD vs both GKHCD and GKHCDVh) and total cholesterol levels (Figure 6E $p < 0.0001$ WSD vs GKHCD and $p < 0.0001$ GKSD vs GKHCD). Interestingly, bromocriptine treatment improved plasma lipid profile by decreasing both plasma triglycerides (Figure 6D $p < 0.001$ vs GKHCD and $p < 0.05$ vs GKHCDVh) and cholesterol levels (Figure 6E $p < 0.001$ vs GKHCD), but no significant changes were observed for plasma free fatty acids (Figure 6F). Such results are in accordance with the lower fat accumulation observed in the liver and pEWAT as well as with increased pEWAT lipid oxidation, as depicted in Figures 3 and 4.

GK rats are described as a model of glucose intolerance and mild fasting hyperglycaemia [16], which was now confirmed by increased glycaemia after 6 h fasting and AUC during the IPITT as presented at Figure 6G,H respectively (Figure 6G $p < 0.0001$ WSD vs GKSD; Figure 6H $p < 0.05$ WSD vs GKSD). The HCD further aggravated such phenotype, by increasing fasting glycaemia (Figure 6G $p < 0.0001$ WSD vs GKHCD and $p < 0.001$ vs GKHCDVh), AUC during the IPITT (Figure 6H $p < 0.0001$ WSD vs GKHCD and $p < 0.001$ vs GKHCDVh) and glycaemia at 1 h during the IPITT (Figure 6I $p < 0.0001$ WSD vs GKHCD and $p < 0.05$ vs GKHCDVh). Conversely, bromocriptine treatment improved glycaemic control by decreasing 6 h fasting glycaemia (Figure 6G) in relation to GKHCD group ($p < 0.01$) and reducing the difference to Wistar rats

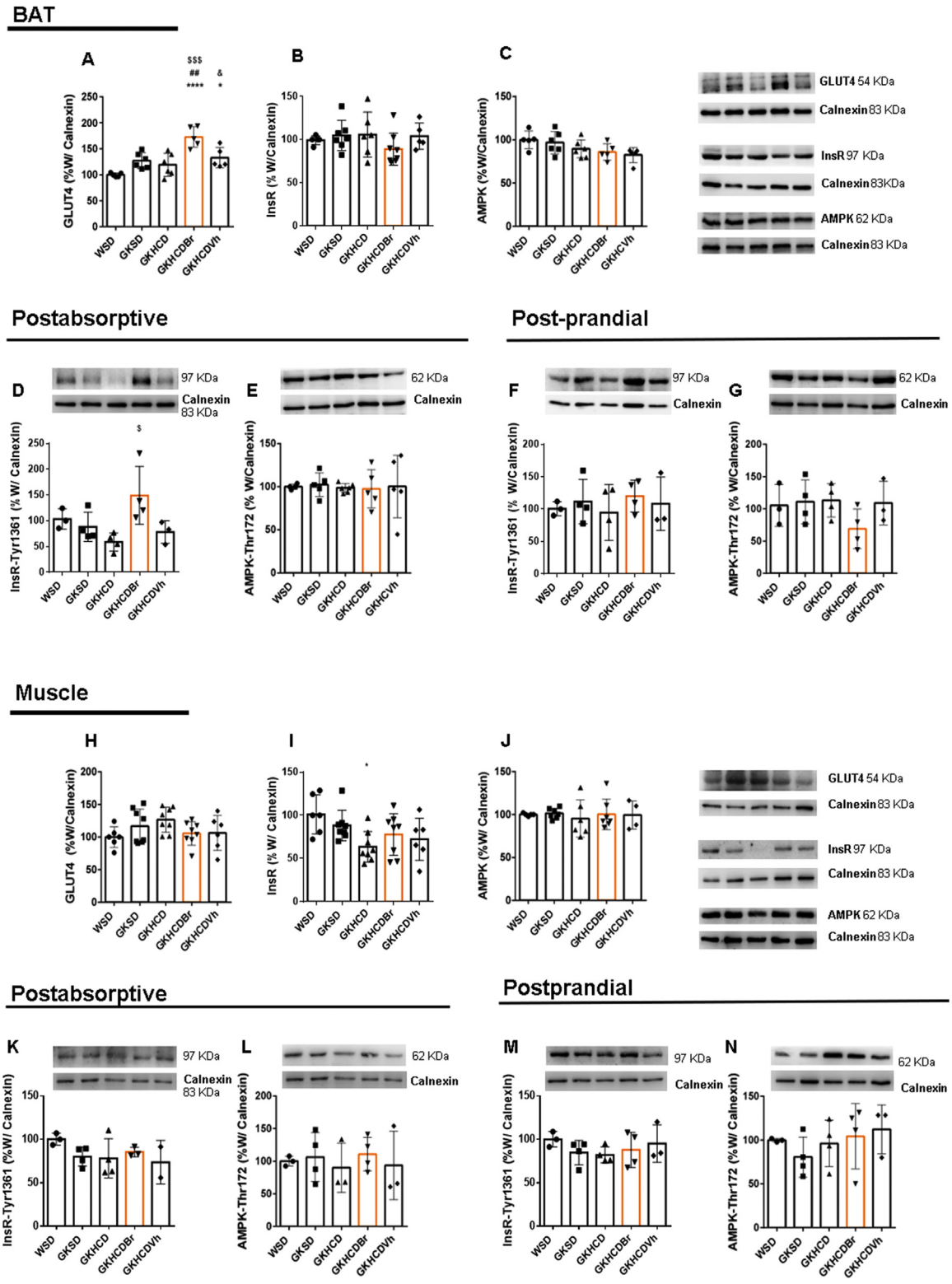

Figure 5: Bromocriptine increased fasting insulin signalling in brown adipose tissue but has no effects in the skeletal muscle. Bromocriptine treatment increased levels of GLUT4 (A) in BAT, while neither InsR (B) nor AMPK (C) levels changed. In the postabsorptive stage increased InsR-Tyr172 (D) after bromocriptine treatment, but no differences were observed for postabsorptive AMPK-Thr172 (E), nor postprandial InsR-Tyr172 (F) and AMPK-Thr172 (G). In the skeletal muscle, no significant changes were observed for GLUT4 (H), InsR (I) total AMPK (J), nor InsR and AMPK activation in the postabsorptive (K, L) or postprandial (M and N) stages. Bars represent means ± standard deviation. One-way ANOVA test with Tukey's multiple comparisons was used to analyse GLUT4, InsR and AMPK total proteins levels; Kruskal—Wallis test was used for IR-Try1361 and AMPK-Thr172 analyses. * Different from WSD; # different from GKSD; $ different from GKHCD; & different from GKHCDBr. Level of significance: 1 symbol, $p < 0.05$; 2 symbols, $p < 0.01$; 3 symbols, $p < 0.001$.

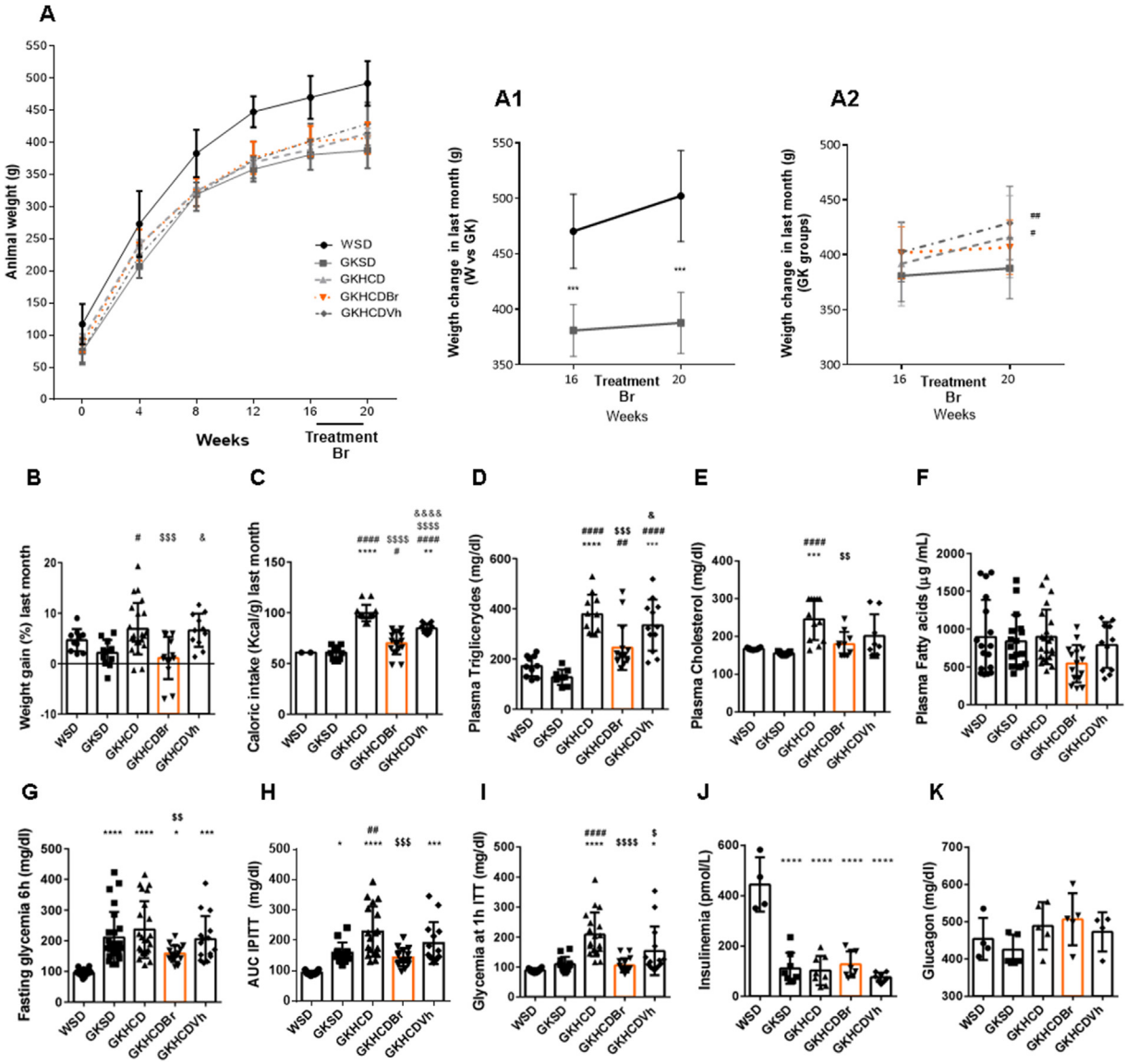

Figure 6: Bromocriptine improves metabolic profile in rats. (A) Weight gain curves during the entire period of the study, and specifically in the last month (A1). Bromocriptine prevented HCD-induced weight gain in the last month (A2 and B). Bromocriptine also reduced caloric intake (C) plasma triglycerides (D) and cholesterol levels (E), without modifying plasma free fatty acids (F). Glucose homeostasis also improved with bromocriptine treatment, namely fasting glycaemia (G), AUC during the ITT (H) and glycemia at 1 h during the IPITT (I), despite no differences were observed in plasma insulin (J) and glucagon levels (K). Values are means ± standard deviation. Differences between groups were assessed by one-way ANOVA test with Tukey's multiple comparisons. * Different from WSD; # different from GKSD; $ different from GKHCD; & different from GKHCDBr. Level of significance: 1 symbol, $p < 0.05$; 2 symbols, $p < 0.01$; 3 symbols, $p < 0.001$.

($p < 0.05$). Moreover, bromocriptine significantly reduced AUC (Figure 6H, $p < 0.001$ vs GKHCD) and glycaemia at 1 h during IPITT (Figure 6I, $p < 0.0001$ vs GKHCD). Plasma insulin levels were decreased in GK rats (Figure 6J, $p < 0.0001$ vs WSD), as consequence of the described β-cell impairment in this animal model [17,18], and remained similar in all the GK groups tested (Figure 6J), as well as glucagon plasma levels (Figure 6K).

4. DISCUSSION

Although the therapeutic effects of the D2R dopaminergic agonist bromocriptine in T2D have been attributed to central actions, peripheral dopamine is acknowledged to directly modulate glucose uptake in insulin-sensitive tissues and lipid metabolism in white adipose tissue. Herein, we hypothesized that patients with T2D may have an impairment of adipose tissue dopaminergic system, which may be a therapeutic target for bromocriptine in T2D patients. We showed that IR patients exhibit a downregulation of *DRD4* and *DRD1* expression in the adipose tissue, which is correlated with markers of adipocyte metabolic function. Additionally, we found in an animal model of T2D and HCD-induced obesity, that bromocriptine remodelled the dopaminergic system of white adipose tissue and the liver, through increased D1R and TH levels. Such mechanisms were associated with higher catabolic function, namely lipid oxidation, and insulin sensitivity in adipose tissue, as well as

lower hepatic steatosis. Importantly, no effects were observed in skeletal muscle and BAT, suggesting a predominant action of bromocriptine in the white adipose tissue.

Borcherding et al., have shown the presence of dopamine receptors in human adipocytes, specifically in the subcutaneous adipose tissue of healthy volunteers [10]. Similar to our results, they showed that the D1R was the most expressed receptor subtype in white adipose tissue, while dopamine receptors type 2 (D2R and D4R) were the less expressed [10]. In the present study, no expression of D3R and D5R was observed, which may be attributed to their absence or very reduced expression or to technical hints, as the selected primers. Nevertheless, similar observations were made by Borcherding et al., who also did not find expression of these two receptors in the subcutaneous adipose tissue [10]. Importantly, similarly to our findings, the same authors found a higher expression of D1R in adipocytes than stromovascular fraction and a 10-fold difference between D1R and D2R expression. In the present study, we showed for the first time, a dysregulation of dopamine receptors expression in the visceral adipose tissue from patients with IR and T2D. It is known that dopamine is involved in the regulation of GSIS, decreasing insulin secretion through D2R-dependent mechanisms [19,20]. It has also been proposed that dopamine-induced decrease of GSIS could be a protective mechanism to avoid β-cell exhaustion [8,21]. Accordingly, it has been reported that obese humans present reduced dopamine levels and/or function, which may be related to the compensatory hyperinsulinemia usually observed in such patients [22]. Herein, we show that IR is a condition also characterized by an imbalance of the dopaminergic system in the adipose tissue, which was correlated with the downregulation of genes implicated in lipid oxidation, *UCP1* and *PPARA*, as well as with *INSR* gene. Given that D1R is a Gs-linked receptor, it is possible that such results reflect lipid oxidation reduction, which leads to lipotoxicity and IR [9,23]. An interesting observation is that lower D1R levels were also found in the pEWAT of T2D rats, confirming the results obtained in human samples and highlighting a translatability of mechanisms between species.

The D2R dopaminergic agonist bromocriptine is the only dopaminergic modulator approved for the treatment of T2D, and it is also commonly used for Parkinson disease and prolactinomas treatment. It was also shown to have insulin sensitizing and beta-cell protecting effects [4,8,24]. To the best of our knowledge, our study is the first to show that chronic bromocriptine treatment leads to an increase in D1R protein levels in both pEWAT and the liver, which may be explained as a possible feedback or balance between the two dopamine receptor families. Importantly, TH protein level also increased with bromocriptine treatment. It is possible that the increased TH levels may reflect increased neuronal dopamine production within the adipose tissue [25], but questions remain whether this is caused by the increase of neuronal projections to the adipose tissue or direct actions of bromocriptine in the tissue. Nevertheless, increased TH levels suggest increased dopamine synthesis in the adipose tissue, possibly released by TH-positive neuron terminals or by the adipocytes themselves, which signals through the D1R to regulate adipocyte metabolism. In fact, the machinery for production of dopamine has been described to be present in adipocytes [10].

The physiological role of higher dopamine synthesis is not well understood. However, the predominant expression of D1R, which is coupled to the Gs protein-cAMP signalling pathway and is further increased by bromocriptine treatment, suggests that D1R can be related to the modulation of catabolic pathways in the pEWAT. Indeed, we have observed increased fasting levels of AMPK-Thr172 and ACL-Ser455 in pEWAT, suggesting higher fasting catabolic activity, towards lipid oxidation. This is in accordance with previous results from our team, showing that the inhibition of D2R by domperidone, when adipose tissue explants were stimulated with dopamine plus insulin, resulted in acute and marked activation of AMPK, ACL and HSL, suggesting a stimulatory effect of D1R on lipid catabolism [12]. Bromocriptine also increased the levels of the InsR and GLUT4 in the pEWAT, as well as the activation of the InsR after the ingestion of a mixed meal. In adipose tissue explants, activation of D2R was shown to acutely potentiate insulin-mediated glucose uptake, which may, nevertheless, denote a role for D2R in the modulation of adipose tissue glucose uptake following bromocriptine treatment [12].

Increased peripheral metabolism in fat depots result not only in a better adipose tissue function, but also in the protection of the liver from lipotoxicity-induced insulin-resistance. Interestingly, herein we found that although the InsR levels were increased in the liver, its postprandial activation was reduced, together with lower AMPK activation. Our group has previously showed that D2R activation by dopamine or bromocriptine induce an acute insulin-independent glucose uptake in liver explants [12]. Here, the observed upregulation of D1R after chronic bromocriptine treatment may result in the opposite effects. Although the liver is expected to significantly contribute to glucose uptake upon a meal ingestion [26], in this study we actually observed lower hepatic GLUT2 levels. Altogether, our results suggest a metabolic remodelling towards a higher metabolic activity in the periphery, and particularly in the white adipose tissue, rather than in the liver, which is consistent with the dramatic decrease of liver fat and adipose tissue weight/adipocyte volume. The marked reduction of steatosis is in line with the observations made by Davis et al. (2006), who also reported lower liver steatosis after Bromocriptine treatment to obese Zucker rats [27]. Importantly, given that no changes were observed in insulin receptor and AMPK activation in the liver, the direct effects of dopamine are questionable. Thus, it is possible that D1R upregulation may be just implicated in lipid mobilization rather than oxidation in the liver. In the adipose tissue, reduced lipotoxicity is associated with postprandial insulin sensitivity and glucose uptake, which is in line with the increment of InsR and GLUT4 levels.

The observed decreased adipose tissue weight is associated with lower leptin levels, which is in accordance with the work by Borcherding et al. showing that modulation of D1R decreased leptin levels both in subcutaneous adipose explants and isolated adipocytes [10]. Moreover, Kok et al., observed decreased plasma leptin levels after bromocriptine treatment in a cohort of obese women [28].

In the present work, it was also possible to observe a metabolic shift in the pEWAT of bromocriptine-treated rats, characterized by higher lipid oxidation rather than glucose utilization in the postabsorptive period and vice-versa in the post-prandial state. This is physiologically relevant and shows that bromocriptine restores the balance of energy supply according to the energetic status and body energy requirement, which may be very important for the prevention of lipotoxicity and glucotoxicity, two hallmarks of insulin resistance and metabolic dysregulation.

Both the BAT and skeletal muscle are considered tissues with higher metabolic rates, since the majority of disposable post-prandial glucose is taken up by the skeletal muscle [29] while BAT converts nutrients energy into chemical energy in the form of heat [30,31]. Both GLUT4 and fasting InsR-Tyr1361 levels were increased in the BAT of bromocriptine-treated animals. We previously showed in BAT explants, that dopamine and bromocriptine exert no direct effects on glucose uptake and InsR and AMPK activation. Thus, our findings obtained herein in the whole-body animal model are likely to result from the overall improvement of the metabolic status and reduction of lipotoxicity, or from other indirect actions of bromocriptine. On the other hand, the activation of D1R in skeletal muscle explants was shown to, directly and independently of insulin, lead to glucose uptake [12]. However, herein no alterations on

dopamine receptors and metabolic pathways were found in the skeletal muscle on the bromocriptine-treated animals. In accordance with the results found herein that show a lack of effect of bromocriptine in skeletal muscle, a clinical trial in obese T2D patients reported that bromocriptine did not improve insulin sensitivity in the skeletal muscle within the physiologic range of hyperinsulinemia [6,29].

As expected, and in accordance with the increased GLUT4 and InsR activation in adipose tissues, bromocriptine treatment resulted in enhanced peripheral insulin sensitivity and improved fasting glycaemia. Particularly, in the study from Pijl et al. (2010), T2D individuals treated with bromocriptine for 16 weeks showed lower fasting glycaemia and improved glucose tolerance tests [32]. Also, bromocriptine treatment in spontaneous hypertensive rats reduced retroperitoneal body fat, C-reactive protein, plasma insulin and glucose levels, and HOMA-IR [33]. Some studies have shown that body weight was unaltered in T2D individuals after bromocriptine administration [28,34,35], which disagrees with our findings. One factor contributing to the lower body weight in our animal model could be the decrease in caloric intake. In fact, it has been shown that bromocriptine treatment restores hypothalamic dopamine levels in rodents, a mechanism shown to be reduced in hibernating animals and involved in insulin resistance during such periods [6,36]. Likewise, Davis et al. (2009) described higher hypothalamic D2R levels after Bromocriptine treatment to obese Zucker rats and associated such increase with reduced hyperphagia and fat mass [37]. However, we could not exclude the possibility of a lower caloric intake in bromocriptine-treated animals due to an improvement in peripheral metabolism or other unknown peripheral actions. In agreement with this, we also found an overall improvement in triglyceride and FFA levels, by diminishing their levels in the liver and their mobilization from adipose tissue to circulation, effects that were also observed in clinical trials [38].

5. CONCLUSION

In summary, our results demonstrate the imbalance of dopamine receptors in visceral adipose tissue from patients with IR, even before glycaemic dysmetabolism. Lower *DRD1* expression correlated with reduced expression of key markers of adipose tissue metabolic function and the *INSR*. Moreover, in an animal model of dysmetabolism, modulation of dopaminergic system through bromocriptine, restored both D1R and TH in white adipose tissue and the liver. Such changes were associated with higher activation of catabolic pathways and lipid oxidation in the adipose tissue during the postabsorptive state and insulin receptor activation in the postprandial state. Altogether, our data suggest that the modulation of peripheral dopaminergic system induces a higher catabolic activity in the white adipose tissue, leading to mobilization of liver lipids, reduced hepatic and adipose tissue lipotoxicity, as well as improved insulin sensitivity and overall metabolic status. Although additional information on the mechanisms involved on dopaminergic regulation of glucose and lipid metabolism should be generated in the future, we can hypothesize that D1R activation could play a role in enhancing metabolic activity. The disclosure of the mechanisms involved in bromocriptine therapeutic effects provide new insights regarding the mechanism of action of bromocriptine in T2D, and highlight the relevance of the modulation of peripheral dopaminergic system for the treatment of metabolic diseases.

ACKNOWLEDGEMENTS

We thank to the at *Laboratório de Biomedicina Mitocondrial e Teranóstica, Centro de Neurociências e Biologia Celular* for the assistance with RNA integrity analysis. We thank the *Serviço de Anatomia Patológica*, Coimbra University Hospital, especially Ilda Simões, for the support with histological techniques.

This work was supported by a grant from GIFT (Grupo de Investigação Fundamental e Translacional) from the Portugal Society of Diabetes and Portugal Foundation for Science and Technology (PEst UID/NEU/04539/2013 and UID/NEU/04539/2019: CNC.IBILI; PEst UIDB/04539/2020 and UIDP/04539/2020: CIBB). G.T and B.F.M. were supported by PhD Grants from the Portuguese Foundation for Science and Technology (PD/BD/127822/2016 and PD/BD/128336/2017, respectively). Bromocriptine was kindly provided by Generis Portugal.

CONFLICT OF INTEREST

The authors have no conflict of interest relevant to this study to declare.

APPENDIX A. SUPPLEMENTARY DATA

Supplementary data to this article can be found online at https://doi.org/10.1016/j.molmet.2021.101241.

REFERENCES

[1] Goossens, G.H., 2007. The role of adipose tissue dysfunction in the pathogenesis of obesity-related insulin resistance. Physiology & Behavior 94(2): 206–218. https://doi.org/10.1016/j.physbeh.2007.10.010.

[2] Guilherme, A., Virbasius, J.V., Puri, V., Czech, M.P., 2008. Adipocyte dysfunctions linking obesity to insulin resistance and type 2 diabetes. Nature Reviews Molecular Cell Biology 9(5):367–377. https://doi.org/10.1038/nrm2391.

[3] Qatanani, M., Lazar, M.A., 2007. Mechanisms of obesity-associated insulin resistance: many choices on the menu. Genes & Development 21(12):1443–1455. https://doi.org/10.1101/gad.1550907.

[4] Roe, E.D., Chamarthi, B., Raskin, P., 2015. Impact of bromocriptine-QR therapy on glycemic control and daily insulin requirement in type 2 diabetes mellitus subjects whose dysglycemia is poorly controlled on high-dose insulin: a pilot study. International Journal of Diabetes Research, 1–7. https://doi.org/10.1155/2015/834903.

[5] Via, M.A., Chandra, H., Araki, T., Potenza, M.V., Skamagas, M., 2010. Bromocriptine approved as the first medication to target dopamine activity to improve glycemic control in patients with type 2 diabetes. Diabetes, Metabolic Syndrome and Obesity: Targets and Therapy(3):43–48.

[6] DeFronzo, R.A., 2011. Bromocriptine: a sympatholytic, D2-dopamine agonist for the treatment of type 2 diabetes. Diabetes Care 34(4):789–794. https://doi.org/10.2337/dc11-0064.

[7] Chamarthi, B., Cincotta, A.H., 2017. Effect of bromocriptine-QR therapy on glycemic control in subjects with type 2 diabetes mellitus whose dysglycemia is inadequately controlled on insulin. Postgraduate Medical Journal 129(4): 446–455. https://doi.org/10.1080/00325481.2017.1315290.

[8] de Leeuw van Weenen, J.E., Parlevliet, E.T., Maechler, P., Havekes, L.M., Romijn, J.A., Ouwens, D.M., et al., 2010. The dopamine receptor D2 agonist bromocriptine inhibits glucose-stimulated insulin secretion by direct activation of the α2-adrenergic receptors in beta cells. Biochemical Pharmacology 79(12):1827–1836. https://doi.org/10.1016/j.bcp.2010.01.029.

[9] Lopez Vicchi, F., Luque, G.M., Brie, B., Nogueira, J.P., Garcia Tornadu, I., Becu-Villalobos, D., 2016. Dopaminergic drugs in type 2 diabetes and glucose homeostasis. Pharmacological Research 109:74–80. https://doi.org/10.1016/j.phrs.2015.12.029.

[10] Borcherding, D.C., Hugo, E.R., Idelman, G., De Silva, A., Richtand, J., Ben-Jonathan, N., et al., 2011. Dopamine receptors in human adipocytes: expression and functions. PloS One 6(9):e25537. https://doi.org/10.1371/journal.pone.0025537.

[11] Vargovic, P., Ukropec, J., Laukova, M., Cleary, S., Manz, B., Pacak, K., et al., 2011. Adipocytes as a new source of catecholamine production. FEBS Letters 585(14):2279–2284. https://doi.org/10.1016/j.febslet.2011.06.001.

[12] Tavares, G., Melo, B.F., Martins, F.O., Matafome, P., Conde, S.V., 2020. Dopamine acts through distinct mechanisms in liver, adipose tissue and skeletal muscle regulating glucose uptake and insulin receptor and AMPK phosphorylation. Diabetologia 63(SUPPL 1). https://doi.org/10.1007/s00125-020-05221-5. S239-S239.

[13] Rodrigues, T., Borges, P., Mar, L., Marques, D., Albano, M., Eickhoff, H., et al., 2020. GLP-1 improves adipose tissue glyoxalase activity and capillarization improving insulin sensitivity in type 2 diabetes. Pharmacological Research 161.

[14] Matafome, P., Santos-Silva, D., Crisóstomo, J., Rodrigues, T., Rodrigues, L., Sena, C., et al., 2012. Methylglyoxal causes structural and functional alterations in adipose tissue independently of obesity. Archives of Physiology and Biochemistry 118(2):58–68. https://doi.org/10.3109/13813455.2012.658065.

[15] Rodrigues, T., Matafome, P., Seiça, R., 2013. Methylglyoxal further impairs adipose tissue metabolism after partial decrease of blood supply. Archives of Physiology and Biochemistry 119(5):209–218. https://doi.org/10.3109/13813455.2013.812121.

[16] Rodrigues, T., Matafome, P., Sereno, J., Almeida, J., Castelhano, J., Gamas, L., et al., 2017. Methylglyoxal-induced glycation changes adipose tissue vascular architecture, flow and expansion, leading to insulin resistance. Scientific Reports 7(1):1698. https://doi.org/10.1038/s41598-017-01730-3.

[17] Almon, R., Wang, X., DuBois, D.C., Cao, Y., Jusko, W.J., 2014. Diabetes disease progression in Goto-Kakizaki rats: effects of salsalate treatment. Diabetes, Metabolic Syndrome and Obesity: Targets and Therapy(7):381–389. https://doi.org/10.2147/DMSO.S65818, 2014.

[18] Movassat, J., Bailbé, D., Lubrano-Berthelier, C., Picarel-Blanchot, F., Bertin, E., Mourot, J., et al., 2008. Follow-up of GK rats during prediabetes highlights increased insulin action and fat deposition despite low insulin secretion. American Journal of Physiology. Endocrinology and Metabolism 294(1):E168–E175. https://doi.org/10.1152/ajpendo.00501.2007.

[19] Farino, Z.J., Morgenstern, T.J., Maffei, A., Quick, M., De Solis, A.J., Wiriyasermkul, P., et al., 2019. New roles for dopamine D2 and D3 receptors in pancreatic beta cell insulin secretion. Molecular Psychiatry. https://doi.org/10.1038/s41380-018-0344-6.

[20] Chaudhry, S., Bernardes, M., Harris, P.E., Maffei, A., 2016. Gastrointestinal dopamine as an anti-incretin and its possible role in bypass surgery as therapy for type 2 diabetes with associated obesity. Minerva Endocrinologica 41(1):43–56.

[21] Roden, M., Shulman, G.I., 2019. The integrative biology of type 2 diabetes. Nature 576(7785):51–60. https://doi.org/10.1038/s41586-019-1797-8.

[22] Wang, G.J., Volkow, N.D., Logan, L., Pappas, N.R., Wong, C.T., Zhu, W., et al., 2001. Brain dopamine and obesity. The Lancet 357(9253):354–357. https://doi.org/10.1016/S0140-6736(00)03643-6.

[23] Nash, A.I., 2017. Crosstalk between insulin and dopamine signaling: a basis for the metabolic effects of antipsychotic drugs. Journal of Chemical Neuroanatomy 83:59–68. https://doi.org/10.1016/j.jchemneu.2016.07.010.

[24] Beaulieu, J.-M., Borrelli, E., Carlsson, A., Caron, M.G., Civelli, O., Espinoza, S., et al., 2019. Dopamine receptors (version 2019.4) in the IUPHAR/BPS guide to pharmacology database. *IUPHARBPS guide pharmacol.* CITE(4). https://doi.org/10.2218/gtopdb/F20/2019.4, 2019.

[25] Pirzgalska, R.M., Seixas, E., Seidman, J.S., Link, V.M., Sánchez, N.M., Mahú, I., et al., 2017. Sympathetic neuron–associated macrophages contribute to obesity by importing and metabolizing norepinephrine. Nature Medicine 23(11):1309–1318. https://doi.org/10.1038/nm.4422.

[26] Adeva-Andany, M.M., Pérez-Felpete, N., Fernández-Fernández, C., Donapetry-García, C., Pazos-García, C., 2016. Liver glucose metabolism in humans. Bioscience Reports 36(6):e00416. https://doi.org/10.1042/BSR20160385.

[27] Davis, L.M., Pei, Z., Trush, M.A., Cheskin, L.J., Contoreggi, C., McCullough, K., et al., 2006. Bromocriptine reduces steatosis in obese rodent models. Journal of Hepatology 45:439–444.

[28] Kok, P., Roelfsema, F., Frolich, M., van Pelt, J., Meinders, A.E., Pijl, H., 2006. Activation of dopamine D2 receptors lowers circadian leptin concentrations in obese women. Journal of Clinical Endocrinology & Metabolism 91(8):3236–3240.

[29] DeFronzo, R.A., Tripathy, D., 2009. Skeletal muscle insulin resistance is the primary defect in type 2 diabetes. Diabetes Care 32(suppl_2):S157–S163. https://doi.org/10.2337/dc09-S302.

[30] Kajimura, S., Seale, P., Spiegelman, B.M., 2010. Transcriptional control of Brown fat development. Cell Metabolism 11(4):257–262. https://doi.org/10.1016/j.cmet.2010.03.005.

[31] Berry, D.C., Stenesen, D., Zeve, D., Graff, J.M., 2013. The developmental origins of adipose tissue. Development 140(19):3939–3949. https://doi.org/10.1242/dev.080549.

[32] Pijl, H., Ohashi, S., Matsuda, M., Miyazaki, Y., Mahankali, A., Kumar, V., et al., 2000. Bromocriptine: a novel approach to the treatment of type 2 diabetes. Diabetes Care 23(8):1154–1161. https://doi.org/10.2337/diacare.23.8.1154.

[33] Kamath, V., Jones, C.N., Yip, J.C., Varasteh, B.B., Cincotta, A.H., Reaven, G.M., et al., 1997. Effects of a quick-release form of bromocriptine (ergoset) on fasting and postprandial plasma glucose, insulin, lipid, and lipoprotein concentrations in obese nondiabetic hyperinsulinemic women. Diabetes Care 20(11):1697–1701.

[34] Kok, P., Roelfsema, F., Frölich, M., van Pelt, J., Stokkel, M.P.M., Edo Meinders, A., et al., 2006. Activation of dopamine D2 receptors simultaneously ameliorates various metabolic features of obese women. American Journal of Physiology. Endocrinology and Metabolism 291(5):E1038–E1043. https://doi.org/10.1152/ajpendo.00567.2005.

[35] Gaziano, J.M., Cincotta, A., O'Connor, C., Ezrokhi, M., Ma, Z.J., Scranton, R.E., et al., 2010. Randomized clinical trial of quick-release bromocriptine among patients with type 2 diabetes on overall safety and cardiovascular outcomes. Diabetes Care 33(7):1503–1508.

[36] Ezrokhi, M., Luo, S., Trubitsyna, Y., Cincotta, A.H., 2014. Neuroendocrine and metabolic components of dopamine agonist amelioration of metabolic syndrome in SHR rats. Diabetology & Metabolic Syndrome 6(1):104. https://doi.org/10.1186/1758-5996-6-104 [37].

[37] Davis, L.M., Michaelides, M., Cheskin, L.J., Moran, T.H., Aja, S., Watkins, P.A., et al., 2009. Bromocriptine administration reduces hyperphagia and adiposity and differentially affects dopamine D2 receptor and transporter binding in leptin-receptor-deficient zucker rats and rats with diet-induced obesity. Neuroendocrinology 89(2):152–162. https://doi.org/10.1159/000170586.

[38] Scranton, R., Cincotta, A., 2010. Bromocriptine–unique formulation of a dopamine agonist for the treatment of type 2 diabetes. Expert Opinion on Pharmacotherapy 11(2):269–279. https://doi.org/10.1517/14656560903501544.

